Astron. Astrophys. 354, 236–246 (2000)

ASTRONOMY AND ASTROPHYSICS

Parsec-scale molecular H_2 outflows from young stars

Jochen Eislöffel⋆

Thüringer Landessternwarte Tautenburg, Sternwarte 5, 07778 Tautenburg, Germany

Received 13 September 1999 / Accepted 2 December 1999

Abstract. Deep imaging in the 1-0 S(1) line of molecular hydrogen was used to search for parsec-scale molecular outflows in L1448, NGC 2071, and NGC 7129. Apart from seven parsec-scale flows, 21 other, shorter molecular outflows were found. This means that on average 25% of the molecular flows are of parsec-scale length, with a variation from 17 to 50% in the three observed regions.

For the 28 outflows, only eight driving sources could be identified with near-infrared sources or nebulosity in our images. Six further sources likely are known deeply embedded Class 0 objects, while for 14 flows no sources could be identified. Therefore, these objects presumably are also deeply embedded, and are good Class 0 candidates.

We find no evidence for different absolute lengths of the parsec-scale molecular flows from known Class 0 and Class I sources in the observed regions, i.e. the length of these flows is not indicative of their true age. These flows have broken out of their cloud cores and likely are moving through a medium too tenuous to produce further visible shock emission. Moreover, even for the flows from the Class 0 sources we derive kinematical ages of up to 2×10^4 years, comparable to the lifetime of these sources, and indicating that outflow activity must start very early in the Class 0 phase of star formation, or even before.

Four molecular H_2 outflows with a high degree of curvature are found in our sample, and mechanisms for their bending are discussed.

Key words: shock waves – molecular processes – stars: formation – ISM: jets and outflows

1. Introduction

Recently has it been found that outflows from young stars can reach parsec-scale lengths. Several such flows have been observed as highly-collimated jets and Herbig-Haro objects in the optical (e.g., Bally & Devine 1994, Eislöffel & Mundt 1997, Reipurth et al. 1997, Devine et al. 1999), or as molecular (CO) outflows at mm-wavelengths (e.g., Bence et al. 1996). Shocks that result from violent internal interactions in a fast jet, or of the jet with the ambient cloud, are thought to excite the gas, so that the flows become visible. Over their lifetimes of several 10^4 years (Eislöffel & Mundt 1997), such flows are able to transfer large amounts of momentum to the surrounding medium. Therefore in sufficient numbers they may be able to shred their parental molecular clouds, and thus stop further star formation activity.

What is the best way to carry out a census for such giant flows? Searches in CO do not suffer from extinction, but usually have a much lower spatial resolution (of $15''$ to $60''$) than optical observations ($1''$). Therefore, in a "crowded" region several smaller flows seen in projection "on top" of each other may mimic one large-scale CO outflow. Observations in the molecular hydrogen lines in the near-infrared, on the other hand, give a high spatial resolution as optical observations, and at the same time are able to penetrate the high extinction in dark clouds to detect these molecular flows (Davis & Eislöffel 1995, Stanke et al. 1998). Also, one can hope to detect flows from sources that themselves are not visible even at near-infrared wavelengths, because they are too deeply embedded. Among such sources one stands high chances to find Class 0 sources, the youngest stellar objects, of which only a few are currently known.

To search for parsec-scale flows among molecular outflows, and to identify their sources, deep imaging in the 1-0 S(1) line of molecular hydrogen at 2.12 μm was carried out in the three star forming regions L1448, NGC 2071, and NGC 7129. Our observations and data reduction are described in Sect. 2. In Sects. 3 – 5 we present molecular outflows and their likely sources in the three observed star forming regions. Implications of our findings are discussed in Sect. 6.

2. Observations and data reduction

The data were obtained in September 1997 using the near-infrared camera MAGIC (Herbst et al. 1993) on the 3.5-m telescope at Calar Alto, Spain. MAGIC is equipped with a 256 × 256 pixel NICMOS3 array, which with the wide-field optics yielded a $0\farcs81$ / pixel scale. For imaging the outflows a narrow-band H_2 ν = 1-0 S(1) filter (λ = 2.122 μm, $\delta\lambda$ = 0.019 μm) was employed. Continuum images for identification and compari-

Send offprint requests to: Jochen Eislöffel (jochen@tls-tautenburg.de)

⋆ Visiting Astronomer, German-Spanish Astronomical Centre, Calar Alto, operated by the Max-Planck-Institute for Astronomy, Heidelberg, jointly with the Spanish National Commission for Astronomy.

son purposes were taken through a H_2 line-free narrow-band filter (λ = 2.1393 μm, $\delta\lambda$ = 0.0201 μm) for NGC 2071, while a K′ filter was used for L1448 and NGC 7129.

The data were flatfielded using dome flat lamp on/off pairs, and sky-subtracted, corrected for bad pixels and cosmics, and mosaiced. No flux calibration was attempted because weather conditions were not photometric during some of the observing time. The coadded integration times are more than 25 min towards the centre of the L1448 and NGC 7129 mosaics and about 10 min towards the edges of these fields. For NGC 2071, the integration time towards the centre of the mosaic is about 5 min, and towards the edges about 2 min.

3. L1448

The extremely high-velocity outflow in L1448 was found by Bachiller et al. (1990). This clumpy flow is highly collimated within 10″ of its source L1448-mm (Guilloteau et al. 1992). It has been extensively imaged in the near-infrared 1-0 S(1) line of molecular hydrogen at 2.12 μm (Bally et al. 1993, Davis et al. 1994, Davis & Smith 1995), and studied spectroscopically (Davis & Smith 1996). Apart from L1448-mm, also called L1488 C, several other deeply embedded sources have been found in the region in far-infrared and mm observations. About 1.′5 north of L1488 C a group of three probable Class 0 objects has been detected (Barsony et al. 1998). The infrared source IRS2, located about 3.′5 northwest of L1488 C was also recognized as a likely Class 0 source recently (O'Linger et al. 1999). Another 3′ to the northwest lies the red nebulous object 13 (RNO 13, Cohen 1980), east of which several knots can be seen on the K′ image of Hodapp (1994). Searches in the optical for Herbig-Haro objects have revealed several objects in L1448 (Eiroa et al. 1994, Bally et al. 1997). In addition to HH 194 – HH 197 in the central part of the molecular cloud, they found four more objects (HH 193, 267, 268, 277) in its outskirts.

3.1. Molecular outflows in L1448

An overview over the central part of the L1448 cloud in the 1-0 S(1) line of H_2 + cont. is shown in Fig. 1. Emission knots belonging to several molecular outflows are spread over this region. In the lower left corner the well-studied outflows from L1488 C and the L1448 North group of sources are seen as the brightest emission line objects in the field. From them, fainter emission knots and filaments extend to the northwest to the positions of the optical Herbig-Haro objects HH 196D and HH 196. HH 196 appears as a large bow shock, stretching over about 1′, with a bright knot at its tip. Very faint diffuse emission may be seen continuing northwest of it. Parallel to this flow, a second flow is seen on its southwestern side. Larger knots in this flow are labelled R and S, in continuation of the naming scheme of Davis & Smith (1995).

Two flows are seen in the western part of the mosaic. The first one is stretching over 6′ in southeast–northwest direction. This line of knots shows a gap near the position of IRS2. The knots south of this gap are bow-shaped and are pointing in a southeasterly direction. Northwest of this gap the flow seems to open up into two strands, which delineate a 2′ long cavity before they join again in HH 195. In the H_2 emission HH 195 exhibits a conical shape, stretching over about 1.′5, before it ends in a bright knot at its apex. Another faint condensation is seen about 1′ beyond this apex to the northwest. The second outflow in this region is oriented in east–west direction. It is seen as a broad band of knots filling the area between the first flow and the RNO 13 reflection nebula east of IRS1. Close to its eastern end the knots of this second outflow are seen in projection onto the first outflow. A kinematical study will be necessary to discern to which flow the individual knots in this region are belonging.

Fig. 2 shows a close-up of the well-studied L1448 molecular outflow. Most prominent in the 1-0 S(1) line of H_2 + cont. is the bipolar flow from L1488 C, with its curved northern and southern outflow lobes. Around the L1448 North group of embedded sources several so far unknown emission features are seen in Fig. 2. A jet-like emission extends to the northwest of L1448 NB. It has been labelled Q in continuation of the naming scheme of Davis & Smith (1995). This emission finger is seen over about 30″, getting progressively fainter to the northwest. The bow-shaped knot P, west of L1448 NW, may be its continuation. North of L1448 NW, there is a larger patch of diffuse emission with several condensations, labelled N. East of L1448 NA and L1448 NW another faint emission feature, labelled O, is seen. It consists of two well-defined condensations at its eastern end, and fainter spread-out emission west of these condensations. A string of emission knots (X, V, U) running parallel to the northern lobe of the L1488 C outflow was identified by Davis & Smith (1995) as an independent flow. This string of knots is continued by another faint knot, labelled M, about 30″ east of the southern lobe of the L1488 C outflow.

3.2. Outflow sources in L1448

There are five known embedded very young sources of Class 0 type and one infrared source (IRS1) in the L1448 cloud. All of these six young stellar objects are likely to drive bipolar molecular outflows. Obviously, the two protostars L1448 C and IRS2 are driving such flows. The northern lobes of these flows start very close to the respective source, with bow-shaped knots pointing to the north(west) (see Fig. 1). South of these two sources, knots begin to appear after a gap of about 30″, with their bows pointing in a southerly direction. IRS1 seems to be the driving source of the east–west outflow in the western part of L1448. This flow lies on the axis of the reflection nebula RNO 13, with IRS1 at its apex. On the counterside, no H_2 emission could be found within 2′ from IRS1 to the limit of our mosaic, but little further away there is HH 194, also lying on the flow axis.

Disentangling the outflows in the L1448 North group of sources is not as unambiguously possible from the available data. The jet-like feature Q emanates from the L1448 NB source (see Fig. 2). HH 196D and HH 196 seem to be the extension of this feature. From L1448 NB, they are seen at a position angle of about 310°, which is coinciding with the position angle of

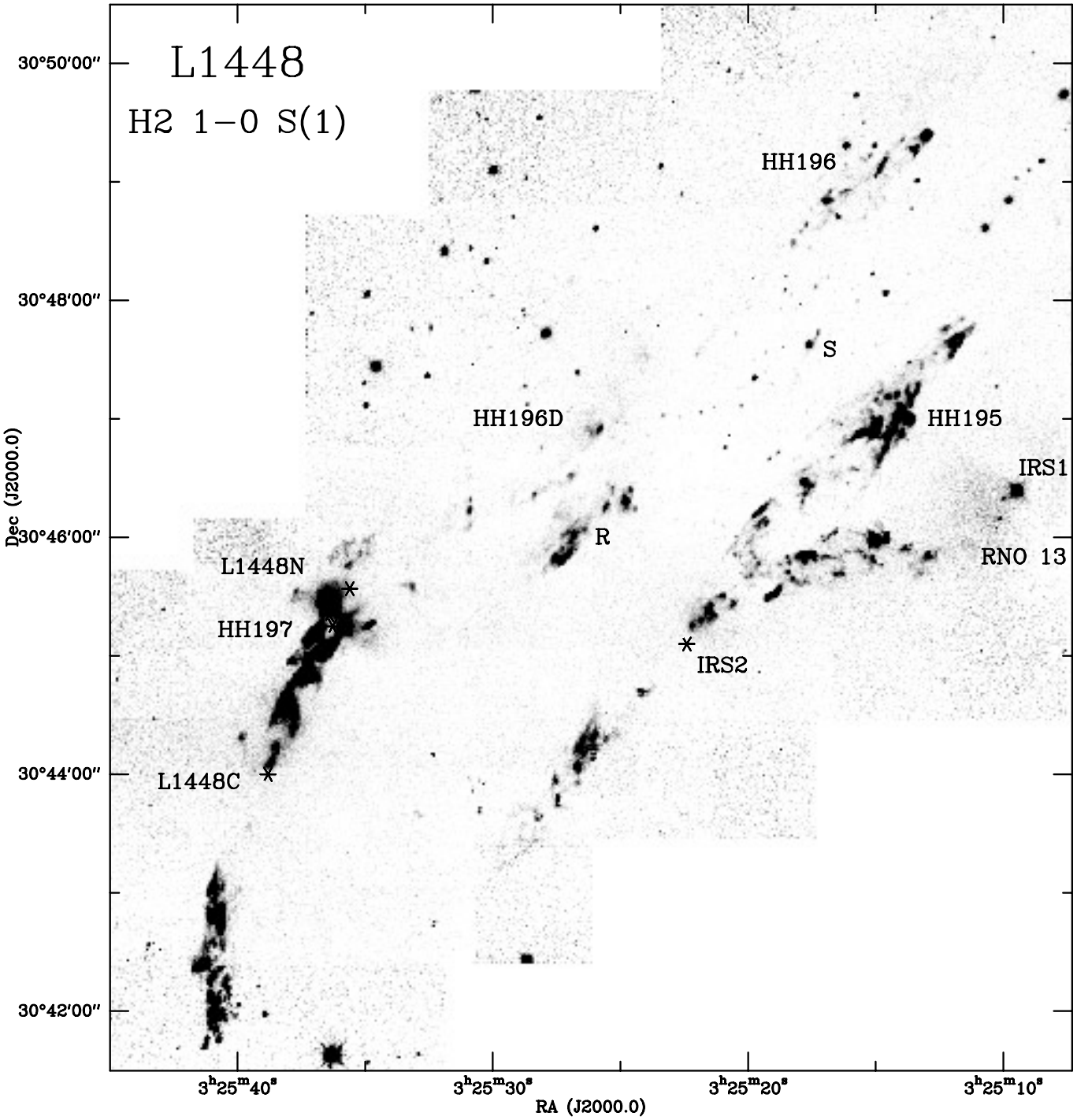

Fig. 1. Mosaic of L1448 in the 1-0 S(1) line of H_2 + cont. at 2.12 μm. Emission knots from several molecular outflows cover much of the area. Positions of embedded sources are marked by a $\star$. H_2 counterparts of optical Herbig-Haro objects are also labelled.

feature Q to within less than 2°. The flow including knots R and S (see Fig. 1) could, however, be an extension of the bending northern L1448 C outflow lobe beyond knot I. The flow east of this lobe and running parallel to it (comprising, among others, knots X, V, U) has been attributed to IRS3 (Davis & Smith 1995), which we now know to consist of L1448 NA, NB, and NW (Barsony et al. 1998). From the morphology of the emission L1448 NA seems to be the most likely source for these knots. The patch of emission N would then be the northern lobe of this outflow. Alternatively, knots X and V could also form the southern lobe of the flow from L1448 NB. Kinematical information is necessary to decide between these possibilities. Such information may then also clarify to which of the two flows the knots U and M further south are belonging. The last remain-

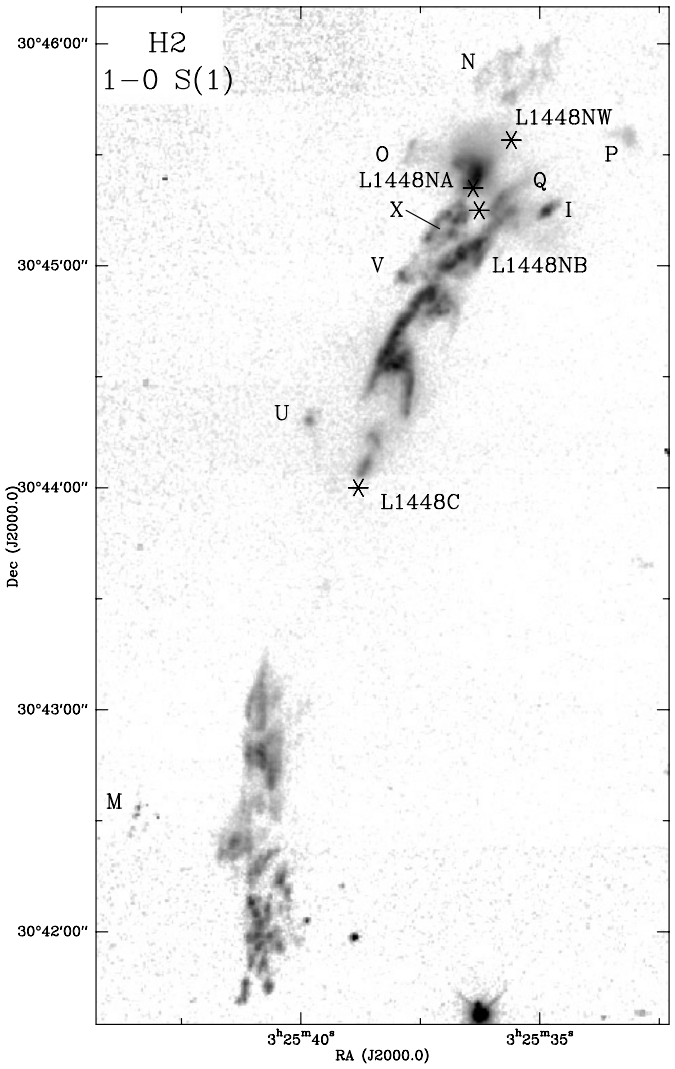

Fig. 2. Close-up of the L1448 C and L1448 N outflow region in the 1-0 S(1) line of H_2 + cont. Known embedded young stellar objects are marked by a $\star$ and are labelled. Also some H_2 emission knots are labelled.

ing embedded object is L1448 NW. It may be driving a flow in east–west direction, with knot O forming the eastern lobe. On the western side, knot P could form part of this flow, although from the orientation of this bow it seems more likely to belong to either the L1448 C or the L1448 NB outflow.

Thus, our new H_2 mosaic of L1448 shows evidence that all of the six known young stellar objects in this cloud are driving an outflow.

4. NGC 2071

The powerful molecular outflow about 4′ north of the NGC 2071 reflection nebula was found by Bally (2) and has been mapped in CO by Snell et al. (1984) and Moriarty-Schieven et al. (1989). Later, it has also been studied in SO, SiO and HCO^+ (e.g., Chernin & Masson 1992,1993). In the near-infrared, molecular hydrogen in its 1-0 S(1) emission line was observed by Lane & Bally (1986), Burton et al. (1989), Garden et al. (1990), and Aspin et al. (1992). Continuum imaging and spectroscopy at near-infrared wavelengths by Walther et al. (1991,1993) have revealed a cluster of infrared sources near the centre of this outflow. Recently, Torrelles et al. (1998) detected two of these infrared sources, IRS1 and IRS3, in the 1.3 cm continuum with the VLA. They found both objects surrounded by H_2O maser spots, and IRS3 to show an ionized thermal bipolar radio jet.

4.1. Molecular outflows in NGC 2071

An overview over the NGC 2071 region in the 1-0 S(1) line of H_2 is presented in Fig. 3. The NGC 2071 reflection nebula is faintly visible in the southern quarter of the field. A multitude of H_2 emission features cover much of the area shown. They have been labelled by roman numerals for convenience. Most prominent is the NGC 2071 North outflow (flow I). Near the centre of the field, it is oriented in northeast–southwest direction. Both flow lobes are filled with filaments and bow-shaped knots, and interspersed diffuse emission. The northwestern lobe, labelled I A, exhibits a curved row of four bright emission knots along its northern wing, which is followed on its outer side by a row of fainter knots offset by a few arcseconds to the north. Further downstream, after a gap of little emission of about 2′, this curved pattern of knots repeats again. In the southwestern lobe, labelled I B, an envelope of diffuse emission is seen around and beyond the bright knots. It is interesting that on this side of the flow a conspicuous edge is seen along the southern wing of the envelope. A second outflow II seems to emanate from close to the centre of the NGC 2071 North flow. It is oriented in east–west direction, with lobes of only about 30″. Nonetheless, its eastern lobe II A is the brightest emission feature in the region, while its western lobe II B is much fainter. Close to the infrared source IRS7 a third flow III is seen. This southeast–northwest oriented flow consists of several fainter filaments extending over about 1′ until it ends in a bright bow-shaped knot. Northeast of it, flow IV stretches parallel to the NGC 2071 North flow. This faint flow starts with a short jet IV A, and, after a gap of about 2′, continues with a group of knots IV B ending in a ring-like structure. Between the second curved knot structure of NGC 2071 North and object IV B, a couple of condensations labelled V are seen, which seem to be oriented in southeast–northwest direction and are probably unrelated to flows I and IV. South of the NGC 2071 North flow lobes two smaller groups of knots are seen in Fig. 3. Flow VI consists of a 20″ long H_2-jet and diffuse emission patches east of two stars. Object VII is a bow-shaped structure with two embedded brighter knots oriented to the south.

A second centre of outflow activity is found in the area of the reflection nebula NGC 2071 in the southern part of Fig. 3. Flow VIII is a 1′ long H_2-jet oriented in east–west direction. This jet consists of several brighter knots near its western end and fades gradually towards the east. The diffuse emission labelled IX north of the jet-like flow VIII is presumably unrelated to it. A further, single knot X of H_2 emission is situated in the northwestern outskirts of the NGC 2071 reflection nebula.

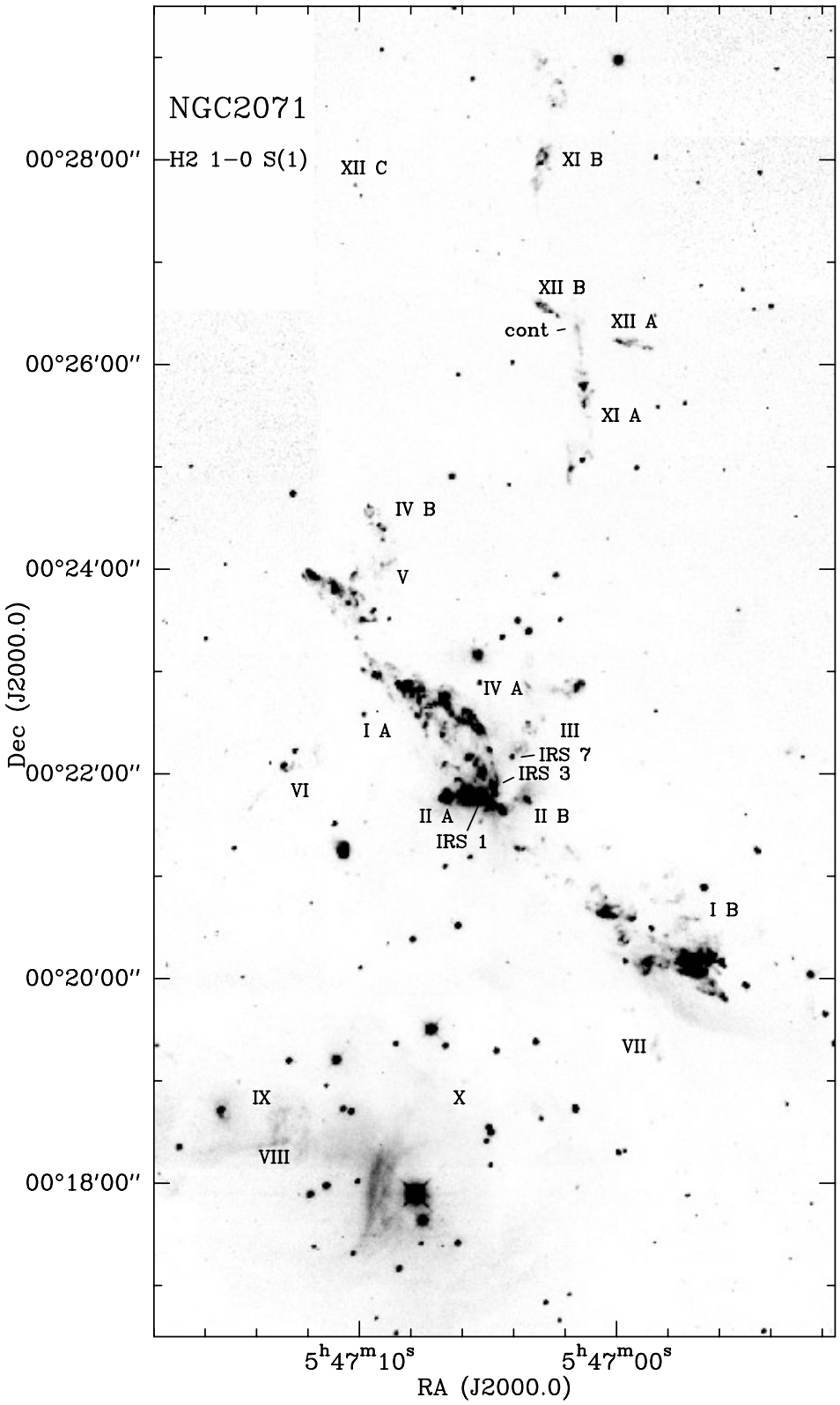

Fig. 3. Mosaic of the NGC 2071 region in the 1-0 S(1) line of H_2 + cont. at 2.12 μm. Several molecular outflows are spread over the field, and are labelled by romal numerals. Also known or suspected outflow sources are marked. The NGC 2071 reflection nebula is faintly seen in the bottom left quarter of the field.

Yet another region of outflow activity is found north of the NGC 2071 North flow. The knotty H_2-jet XI A starts at an elongated continuum knot (marked "cont" in Fig. 3) and extends well-collimated about 1′ southward, where it opens up into a filamentary structure. Beyond these filaments, after a gap of about 6′, the emission knots VII are also situated on the jet axis and are oriented in the same direction. Therefore, they may be part of flow XI as well. On the counterside, over more than 1′

north of the continuum nebulousity other filamentary and ring-like structures XI B are seen, probably forming the counterflow of this long outflow. A second, bending flow XII is crossing the continuum source in northeast–southwest direction. A row of knots to the west, labelled XII A, and to the east of the continuum source, labelled XII B, may continue in a single knot XII C about 2′ further to the northeast.

4.2. Outflow sources in NGC 2071

With the data at hand, driving sources for only a few of the flows in the NGC 2071 region can be identified with some confidence. The detection of a bipolar thermal radio jet from IRS3 oriented in the direction of the NGC 2071 North flow, and of a ring of H_2O maser spots perpendicular to the flow axis by Torelles et al. (1998) strongly suggest that IRS3 is the driving source of the NGC 2071 North flow (flow I). Similarly, the position of IRS1 between the opposing outflow lobes of flow II, and the detection of a ring of H_2O maser spots around this source perpendicular to the flow axis (Torrelles et al. 1998) make IRS1 the likely source of flow II. Furthermore, its position at the southeastern end of flow III indicates that IRS7 is the source of this flow. It seems very likely that the driving source of flow XI is embedded in the continuum nebulosity at the base of the H_2-jet XI A. Moreover, the fact that a connecting line between flow structures XII A and XII B also crosses this continuum nebulosity suggests that the source of this flow may also be hidden in the nebulosity. Since flows XI and XII are seen under a large angle it is unlikely that they are driven by the same source. A young non-coplanar binary system in which each star is driving one of the flows seems to be an interesting alternative. A variety of such systems including T Tau, L1551 IRS5, and HH 24/SVS 63 have recently been studied by Terquem et al. (1999).

Information to pin down the driving sources of the other molecular outflows in the NGC 2071 region (flows IV, V, VI, VII, VIII, IX, X) is not yet available. Many of these sources are presumably still deeply embedded and are not seen at near-infrared wavelengths. Mapping the region in the continuum at mm- or cm-wavelengths will therefore be essential to detect these very young objects.

5. NGC 7129

Two molecular CO outflows were found in NGC 7129 by Edwards & Snell (1983). They seem to be associated with the two far-infrared sources LkHα 234 (also a visible star) and FIRS2 discovered earlier by Bechis et al. (1978). In the optical, a large number of Herbig-Haro objects in and near NGC 7129 have been reported (Hartigan & Lada 1985, Eiroa et al. 1992, Gómez de Castro et al. 1993, Miranda et al. 1993, Gómez de Castro & Robles 1999). Also a highly-collimated optical jet was found to emanate from LkHα 234 (Ray et al. 1990). Molecular hydrogen emission in the near-infrared has been detected from several of the optical Herbig-Haro objects (Wilking et al. 1990). Recently, Eiroa et al. (1998) presented resolution-enhanced IRAS maps of NGC 7129, and with additional (sub-)mm observations identified FIRS2 as an intermediate-mass counterpart of Class 0 objects.

5.1. Molecular outflows in NGC 7129

The field of NGC 7129 in the 1-0 S(1) line of H_2 + cont. at 2.12 μm is shown in Fig. 4. Above the centre of the image we see the stellar cluster of NGC 7129, with LkHα 234, BD+65° 1638 and SVS 13 as its brightest members in the near-infrared. A bright filament of H_2 emission is stretching southward from near LkHα 234, and after about 70″ is bending over to a southwesterly direction. This filament, which we consider as a photodissociation region (PDR), outlines the southeastern edge of an about 4′ long elongated cavity, extending in northeast–southwest direction, with LkHα 234 at its northeastern apex. It is, however, not evident which of the stars in the cluster is responsible for the clearing of this cavity. At its southwestern end we see two bright groups of H_2 emission knots, GGD 32 and HH 103, and several fainter ones. Their orientation indicates that they originate from an outflow from the direction of the stellar cluster. On the opposite side of the cluster there is a very broad flow visible which is directed to the northeast. HH 105 forms a large part of this broken-up flow with many little bow shocks and filaments, and diffuse emission between them. We note, however, that not all of the H_2 emission in this region belongs to a single flow. Projected onto the big flow we are seeing GGD 34. This object (see Fig. 4) consists of a cavity with a continuum nebulousity at its western end, which harbours the driving source. The cavity edges are outlined by H_2 emission, with an emission knot at its eastern end and two other knots about 20″ and 30″ further downstream. Two other groups of knots with unclear origin have been labelled I and II. While the group of knots I on the axis of the large flow could be a further bow shock of this flow, knots II seem to belong to an independant outflow with a more easterly flow direction.

Several other molecular outflows are found in the field of NGC 7129. To the northwest of the stellar cluster a small bipolar outflow with two bow shocks pointing in opposite directions, labelled III A and III B, is seen. Most of the new outflows are, however, found in the region around FIRS2 south of the cluster. A close-up of this region in the 1-0 S(1) line of H_2 + cont. is shown in Fig. 5. Most prominent is the southeast–northwest oriented flow around FIRS2. Surprisingly, the southeastern lobe of this flow is changing direction about 70″ from FIRS2 and is bending southward, while its counterflow is bending westward. The small bow labelled IV could only be part of this flow if it bent even stronger to a southwesterly direction. Two bows pointing in opposite directions labelled V A and V B delineate a flow that is crossing the FIRS2 flow in projection. In the upper left corner of Fig. 5 another prominent jet-like object labelled VI A is seen. After a gap of about 60″ a further bow-shaped knot VI B of this flow was detected. In the area between this f low and the FIRS2 flow another faint, but well-collimated flow VII is seen. In its neighbourhood three more knots, labelled VIII, IX, and X are found. To identify their origin or membership to other flows, information about their kinematics will be necessary.

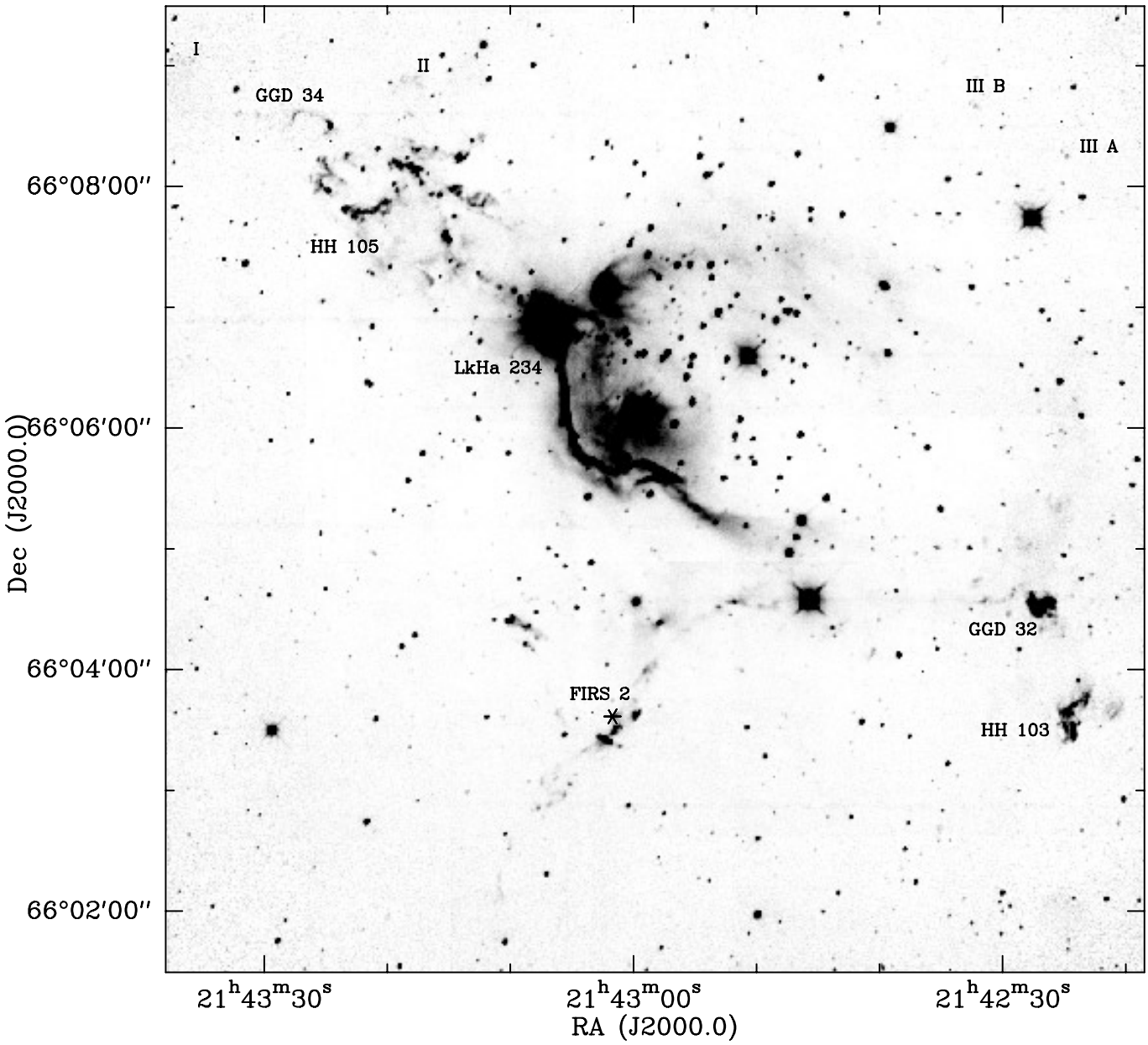

Fig. 4. Mosaic of the NGC 7129 region in the 1-0 S(1) line of H_2 + cont. at 2.12 μm. Emission from several molecular outflows, as well as from a probable photodissociation region to the east and south of the stellar cluster cover the field. Some H_2 outflows and H_2 counterparts of optical Herbig-Haro objects are labelled.

5.2. Outflow sources in NGC 7129

In the NGC 7129 region likely driving sources can be identified for only three flows with the available data. One can be quite confident that the driving source of the GGD 34 flow is residing in the continuum nebulosity at the western end of this object. Also, it seems probable that the embedded object FIRS2 (Eiroa et al. 1998) is the driving source of the extended southeast–northwest oriented flow crossing it. On the axis of the large bipolar flow between HH 103 and HH 105 we find LkHα 234 as a potential driving source. Ray et al. (1990) discovered an optical highly-collimated jet from this star, which is seen under a position angle of 252°, while the large molecular outflow has a position angle of about 235°. This optical jet can be traced, however, only over a short distance compared to the extent of the molecular outflow seen in Fig. 4. Therefore, it seems possible that precession of the source has somewhat changed the direction into which the HH jet is currently pointing, and that LkHα 234 is indeed the source of the large-scale molecular H_2 outflow in NGC 7129.

For most of the other emission-line knots and molecular flows (flows II, III, IV, V, VI, VII, VIII, IX, X) no evident sources are seen in our mosaic (Fig. 4). Mm- or cm-continuum measurements will be necessary to detect embedded candidate driving

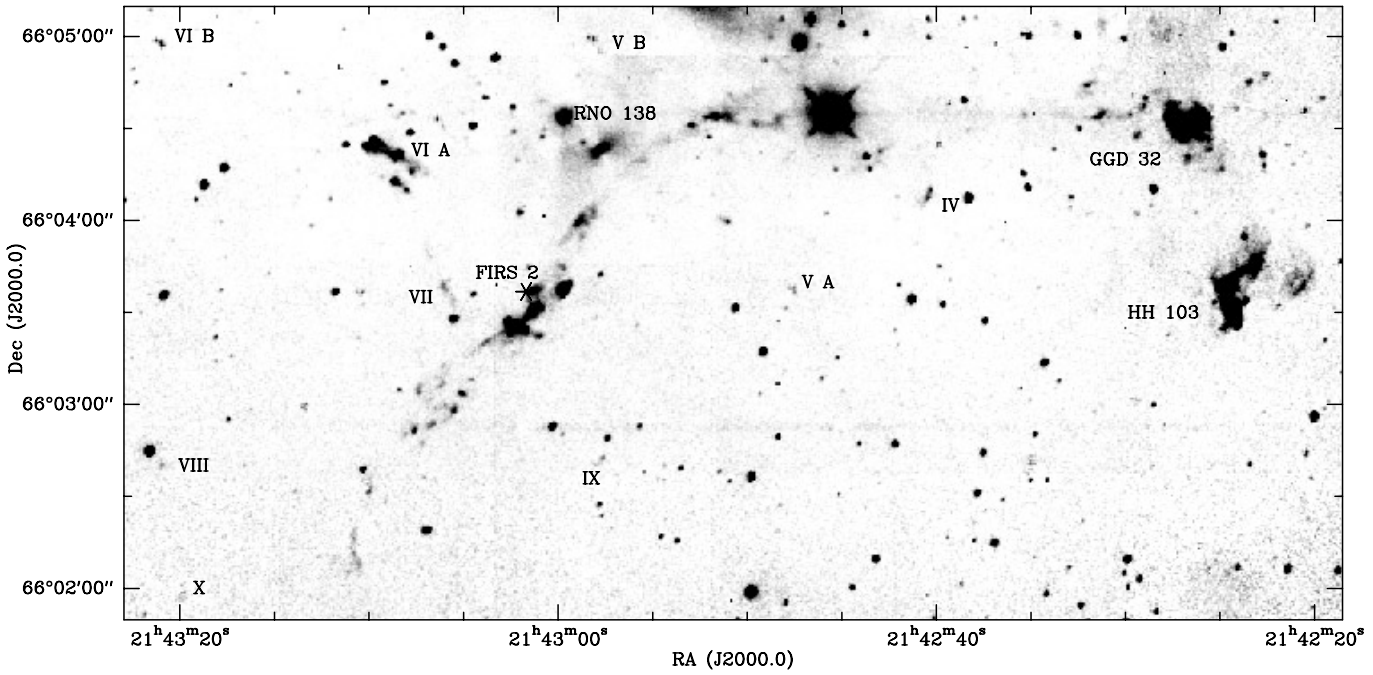

Fig. 5. Close-up of the NGC 7129 FIRS2 region in the 1-0 S(1) line of H_2 + cont. H_2 outflows and emission knots are labelled by roman numerals, counterparts of optically visible objects by their names. The position of FIRS2 is indicated by a $\star$.

sources in this region. We note that no flow has been found from the bipolar nebula RNO 138 (see Fig. 5), which recently has been observed to go through a strong outburst (Miranda et al. 1994).

6. Discussion

6.1. Parsec-scale molecular outflows

It is interesting that in all three observed regions L1448, NGC 2071, and NGC 7129 molecular H_2 outflows of parsec-scale length were observed. In our mosaic of the L1448 cloud, the molecular flow from L1448 NB can be traced from knot M to HH 196, i.e. over 0.87 pc (for a distance of 300 pc to L1448). The bipolar flows from L1448 C and IRS2, on the other hand, are somewhat shorter at 0.71 pc and 0.65 pc, respectively. The lengths of the flows observed in our H_2 mosaic increase drastically when more distant optical Herbig-Haro objects along the flow axes are taken into account (see Bally et al. 1997). Then, the L1448 NB flow reaches a total length of 3.60 pc from HH 193 in the north to HH 278 in the south. Similarly, with a northern lobe out to HH 267 the total length of the IRS2 flow amounts to 2.15 pc. Also the IRS1 flow, with a western lobe reaching to HH 268, would be at least 1.35 pc long.

In NGC 2071, there are two flows that reach lengths of over 1 pc (for a distance to NGC 2071 of 500 pc). One is the prominent NGC 2071 North flow (flow I) with a total length of at least 1.03 pc. The other one is flow XI which extends over as much as 10′ or 1.46 pc from knots XI B to VII. Flow XII, on the other hand, measures only 0.50 pc from knots A to C. Also in NGC 7129, at a distance of 1250 pc (Shevchenko & Yakubov 1989), two flows with lengths over 1 pc are seen. Longest is the prominent NGC 7129 molecular outflow, which from HH 103 in the southwest to knot I in the northeast is seen over almost 10′ or at least 3.54 pc. Second longest, at about 4′ or 1.45 pc is the FIRS2 flow, while flow V from bows V A to V B extends over merely 2′, or 0.67 pc.

It is interesting comparing the frequency of parsec-scale flows among the molecular outflows in the three observed regions. In L1448 at least 3 out of 6, in NGC 2071 at least 2 out of 10, and in NGC 7129 at least 2 out of 12 molecular outflows have parsec-scale lengths, i.e. 17 to 50%, depending on the region. In total we found seven parsec-scale flows out of 28 molecular outflows, or on average 25% in all three regions together. This indicates that outflows, even from very young sources, reach parsec-scale lengths fairly often.

Does the observed length of the flows then increase with age? Three of our seven parsec-scale flows seem to originate from Class I sources (L1448 IRS1, NGC 2071 North flow, NGC 7129 flow), while four originate from Class 0 sources (L1448 NB and IRS2, NGC 2071 XI, NGC 7129 FIRS2). Although we are dealing with small numbers, and we measure only the projected lengths of these flows, no significant differences can be seen neither in the length of the longest Class I flow (NGC 7129 flow, 3.54 pc) versus the longest Class 0 flow (L1448 NB, 3.60 pc), nor in the average length of these parsec-scale flows from Class I sources (2.0 pc) versus those from the Class 0 sources (2.2 pc). Hence, there is no trend visible in the data presented in this paper, that would indicate that older (Class I) flows appeared longer than younger (Class 0) outflows.

In analogy, there will be no difference in the kinematical ages of the flows from these Class 0 and Class I sources. If we assume a constant outflow velocity of 200 km s^{-1}, and do not

take into account possible projection effects (which we cannot estimate for the single sources), we find kinematical ages of about 18000 years for the two longest flows L1448 NB and NGC 7129 flow. Flows of about 1.5 pc length, like L1448 IRS1, NGC 2071 XI, and NGC 7129 FIRS2, still reach kinematical ages of about 7000 years. Thus, kinematical ages of the flows from the Class 0 sources in our sample are of the order of the lifetime of these sources of about 10^4 years. This indicates that outflow activity must start very early during the star formation process, at the beginning of the Class 0 phase, or even before. Consequently, if outflow activity starts early in the Class 0 phase, but at the same time the much older Class 0 sources exhibit flows of about equal length, then total outflow duration apparently is not an important factor for the observed total length of these flows. We note that the typical size of star forming molecular cloud cores is of the order of 0.1 – 0.2 pc (e.g. Falgarone et al. 1998, André et al. 2000). At parsec-scale length, outflows will certainly have broken out of their parental cores. Conceivably, at some distance from the cores the ambient material will get so tenuous that the outflowing gas does not produce visible shock emission any more on its further way out. Therefore, for all outflows that reach beyond this point their traceable flow sections would be of comparable length, independent of their actual length, and their age. Since we see the outflows from Class 0 sources already stretching far beyond the typcial core radius, it seems likely that they reach beyond the point where they become invisible for us. Therefore, they show the same apparent lengths as their older counterparts from Class I sources.

6.2. Clusters of embedded outflow sources

A surprising result of this "mini-survey" for parsec-scale molecular outflows is the detection of a large number of flows in each of the three observed regions. These groups or "clusters" of outflows hint at a corresponding number of young stellar objects which are simultaneously going through the outflow phase of their evolution. It is interesting that only for eight flows driving sources could be identified as near-infrared sources or nebulousity on our images. Another six sources are known as deeply embedded Class 0 objects from mm-observations. For the remaining 14 flows, however, no sources could be identified. Therefore, it is likely that they are all too deeply embedded to be visible in the near-infrared. Hence most of them may be good candidate Class 0 objects, which could be detected with mm- or cm-continuum observations.

In this "mini-survey", on the other hand, for all known Class 0 sources outflows could be identified: In L1448, for example, 5 out of the 6 driving sources are known Class 0 objects. Thus the frequency of outflow activity in NGC 2071 and NGC 7129 also seems to make them good hunting grounds to study the formation of a population of the youngest stellar objects known. Furthermore, the detection of clusters of molecular H_2 outflows in NGC 2071 and NGC 7129 means that the original CO observations with comparatively poor spatial resolution were confused by the various flows, often pointing in different directions. These observations are not well-suited to derive parameters of these flows, nor of the exciting stars and their surroundings. CO observations at higher spatial resolution – resolving the individual flows – are necessary for deriving their characteristics.

6.3. Bending molecular outflows

It is interesting that in all three observed star forming regions bending molecular H_2 outflows are seen. So far, wiggling has been reported in a few molecular outflows, including Cep E (Eislöffel et al. 1996) and in RNO 15 (Davis et al. 1997). Such wiggling has been interpreted in terms of precession of the outflow, caused, e.g., by disk precession in a binary system (Terquem et al. 1999). Here, however, much stronger bending is observed in three molecular outflows: the northern lobe of the L1448 C flow bends by about 35° to the northwest, the NGC 2071 flow XII bends by 25°, and the northern lobe of the NGC 7129 FIRS2 flow bends westward by about 65°, while the southern lobe bends westward by 35°. The only other molecular H_2 outflow showing such strong bending, to our knowledge, was found in S187 by Salas et al. (1998). The bends in the flows presented here, however, show different morphologies. Therefore, they may be caused by different physical processes. Wiggly structure in the lobes of the L1448 C flow (see Fig. 2) can be explained by precession (Dutrey et al. 1997). The strong bend in the northern lobe of this flow, however, has been attributed to deflection of the flow in a collision with a dense clump or another outflow (Bachiller et al. 1995). In NGC 2071, both flow XII and the prominent NGC 2071 North flow do show some bending (Fig. 3). In the latter flow a double pattern of bright knots is seen along the northern wing of the northeastern lobe, while – in point-symmetry – on the counterside the southern wing of the lobe shows a conspicuous edge. Such a structure is expected from a precessing flow, with a precession period longer than the observed part of the flow. Flow XII, on the other hand, shows a kink between knots XII A and XII B, on both sides of the continuum nebulousity. Such a symmetry would be difficult to understand with a precession model. More likely may be the proper motion of the driving source through the dense medium of the cloud. From the observed geometry, and not including any projection effects, one can estimate that the source should be moving at about 10 – 15% of the flow speed perpendicular to the outflow direction. This flow speed has not yet been measured, but assuming a typical flow speed of 200 km s^{-1} the source would move at 20 – 30 km s^{-1} relative to the cloud. This appears fast, but not impossible, e.g. after a close encounter.

The most complicated structure is seen in the NGC 7129 FIRS2 flow (Fig. 5). Here, after a straight flow section of about 70″, both the flow and the counterflow bend over into the same direction! Until kinematic information about this flow has been obtained, it will be difficult to determine the cause of the observed deformation with some certainty. One may speculate if a scenario of a supersonic side-wind could apply, similar to the one suggested for S187 by Salas et al. (1998; see also Cantó & Raga 1995). Then, the NGC 7129 FIRS2 flow should be shielded against such a wind by the dense

cloud core in its inner part, and upon leaving this core should get pushed out of its straight flow direction by a supersonic side-wind. Parameters for the flow and the wind very similar to those calculated for S187 by Salas et al. (1998) (to within a few percent) would also fit the bending of the outer ends of the FIRS2 flow: a jet velocity of $150\,\mathrm{km\,s^{-1}}$ with a mass loss rate of 10^{-7} $M_\odot$/yr and a sound speed in the flow of $10\,\mathrm{km\,s^{-1}}$, and a density of $3\times10^{-20}\,\mathrm{g\,cm^{-3}}$ and a velocity of $10\,\mathrm{km\,s^{-1}}$ for the ambient wind. Such a wind could originate in one of the other young stars in NGC 7129, like LkHα 234.

Currently, the detection of four so strongly curved molecular H_2 flows in three star forming regions (with only one other known in the literature) may seem fortuitous. Similarly deep imaging of other such regions may show how common such flows really are, given that a variety of mechanisms seem to be able to bend a flow without destroying it.

7. Conclusions

Deep imaging in the near-infrared 1-0 S(1) line of H_2 at 2.12 μm was used to search for parsec-scale molecular outflows in the L1448, NGC 2071, and NGC 7129 star forming regions. Seven parsec-scale flows were found in these regions. Surprisingly, also 21 other, shorter molecular flows were detected. This means that on average (at least) 25% of all detected molecular flows are of parsec-scale length, with a variation of this fraction between 17 and 50% in the three observed regions.

Only for eight flows driving sources could be identified as near-infrared sources or nebulousity on our images. A further six likely sources are known as deeply embedded Class 0 objects from mm observations. For the remaining 14 flows no sources could be identified. Presumably these sources are also deeply embedded, and hence are good candiates for Class 0 objects. Mm surveys in the regions should reveals these objects.

We find no evidence for different absolute lengths of the parsec-scale molecular H_2 flows from known Class 0 and Class I sources, i.e. the length of these flows is not indicative of their true age. Since all of these flows are much longer than the typical size of star forming cloud cores, we suggest that after breaking out of the cores they have now reached regions too tenuous to produce shock emission that would make them visible on their further way out.

Moreover, even for the flows from the Class 0 sources we derive kinematical ages of up to 2×10^4 years. Since this is the generally assumed lifetime of Class 0 sources we find that outflow activity must start very early in the Class 0 phase of star formation, or even before.

Among the detected molecular outflows, four show a high degree of curvature. Various mechanisms, like precession, deflection from a dense clump, a supersonic side-wind, or motion of the source through a dense cloud, may be invoked to explain these kinks and bends of partly differing morphology. Ultimately, kinematical information will be necessary to test these various mechanisms.

Acknowledgements. I thank David Devine, the referee, for his helpful comments. This work was partially supported through DFG grant Ei409/1-1.

References

André P., Ward-Thompson D., Barsony M., 2000, In: Mannings V., Boss A.P., Russell S.S. (eds.) Protostars and Planets IV, University of Arizona Press, Tucson, in press
Aspin C., Sandell G., Walther D.M., 1992, MNRAS 258, 684
Bachiller R., Cernicharo J., Martin-Pintado J., Tafalla M., Lazareff B., 1990, A&A 231, 174
Bachiller R., Guilloteau S., Dutrey A., Planesas P., Martin-Pintado J., 1995, A&A 299, 857
Bally J., 1982, ApJ 261, 558
Bally J., Devine D., 1994, ApJ 428, L65
Bally J., Lada E.A., Lane A.P., 1993, ApJ 418, 322
Bally J., Devine D., Alten V., Sutherland R.S., 1997, ApJ 478, 603
Barsony M., Ward-Thompsom D., André P., O'Linger J., 1998, ApJ 509, 733
Bechis K.P., Harvey P.M., Campbell M.F., Hoffmann W.F., 1978, ApJ 226, 439
Bence S.J., Richer J.S., Padman R., 1996, MNRAS 279, 866
Burton M.G., Geballe T.R., Brand P.W.J.L., 1989, MNRAS 238, 1523
Cantó J., Raga A.C., 1995, MNRAS 277, 1120
Chernin L.M., Masson C.R., 1992, ApJ 396, L35
Chernin L.M., Masson C.R., 1993, ApJ 403, L21
Cohen M., 1980, AJ 85, 29
Davis C.J., Eislöffel J., 1995, A&A 300, 851
Davis C.J., Smith M.D., 1995, ApJ 443, L41
Davis C.J., Smith M.D., 1996, A&A 309, 929
Davis C.J., Eislöffel J., Ray T.P., Jenness T., 1997, A&A 324, 1013
Davis C.J., Dent W.R.F., Matthews H.E., Aspin C., Lightfoot J.F., 1994, MNRAS 266, 933
Devine D., Reipurth B., Bally J., Balonek T.J., 1999, AJ 117, 2931
Dutrey A., Guilloteau S., Bachiller R., 1997, A&A 325, 758
Edwards S., Snell R.L., 1983, ApJ 270, 605
Eiroa C., Gomez de Castro A.I., Miranda L.F., 1992, A&AS 92, 721
Eiroa C., Palacios J., Casali M.M., 1998, A&A 335, 243
Eiroa C., Miranda L.F., Anglada G., Estalella R., Torrelles J.M., 1994, A&A 283, 973
Eislöffel J., Mundt R., 1997, AJ 114, 280
Eislöffel J., Smith M.D., Davis C.J., Ray T.P., 1996, AJ 112, 2086
Falgarone E., Panis J.-F., Heithausen A., et al., 1998, A&A 331, 669
Garden R.P., Russell A.P.G., Burton M.G., 1990, ApJ 354, 232
Gómez de Castro A.I., Miranda L.F., Eiroa C., 1993, A&A 267, 559
Gómez de Castro A.I., Robles A., 1999, A&A 344, 632
Guilloteau S., Bachiller R., Fuente A., Lucas R., 1992, A&A 265, L49
Hartigan P., Lada C.J., 1985, ApJS 59, 383
Herbst T.M., Beckwith S.V.W., Birk C., et al., 1993, Proc. SPIE 1946, 605
Hodapp K.-W., 1994, ApJS 94, 615
Lane A.P., Bally J., 1986, ApJ 310, 820
Miranda L.F., Eiroa C., Birkle K., 1994, A&A 289, L7
Miranda L.F., Gómez de Castro A.I., Eiroa C., 1993, A&A 271, 654
Moriarty-Schieven G.H., Hughes V.A., Snell R.L., 1989, ApJ 347, 358
O'Linger J., Wolf-Chase G., Barsony M., Ward-Thompson D., 1999, ApJ 515, 696
Ray T.P., Poetzel R., Solf J., Mundt R., 1990, ApJ 357, L45
Reipurth B., Bally J., Devine D., 1997, AJ 114, 2708
Salas L., Cruz-Gonzalez I., Porras A., 1998, ApJ 500, 853

Shevchenko V.S., Yakubov S.D., 1989, SvA 33, 370
Snell R.L., Scoville N.Z., Sanders D.B., Erickson N.R., 1984, ApJ 284, 176
Stanke T., McCaughrean M.J., Zinnecker H., 1998, A&A 332, 307
Terquem C., Eislöffel J., Papaloizou J.C.B., Nelson R.P., 1999, ApJ 512, L131
Torrelles J., Gómez J.F., Rodríguez L.F., et al., 1998, ApJ 505, 756
Walther D.M., Geballe T.R., Robson E.I., 1991, ApJ 377, 246
Walther D.M., Robson E.I., Aspin C., Dent W.R.F., 1993, ApJ 418, 310
Wilking B.A., Schwartz R.D., Mundy L.G., Schultz A.S.B., 1990, AJ 99, 344